Published for SISSA by Springer

Received: May 19, 2023
Revised: July 14, 2023
Accepted: August 8, 2023
Published: September 1, 2023

A novel unbinned model-independent method to measure the CKM angle γ in $B^{\pm} \to DK^{\pm}$ decays with optimised precision

Jake Lane,[a,b] **Evelina Gersabeck**[b] **and Jonas Rademacker**[c]

[a] *Monash University, Melbourne, Australia*
[b] *University of Manchester, Manchester, U.K.*
[c] *University of Bristol, Bristol, U.K.*

E-mail: jake.lane@cern.ch, evelina.gersabeck@cern.ch, jonas.rademacker@bristol.ac.uk

Abstract: We present a novel unbinned method to combine $B^{\pm} \to DK^{\pm}$ and charm threshold data for the amplitude-model unbiased measurement of the CKM angle γ in cases where the D meson decays to a three-body final state. The new unbinned approach avoids any kind of integration over the D Dalitz plot, to make optimal use the available information. We verify the method with simulated signal data where the D decays to $K_S\pi^+\pi^-$. Using realistic sample sizes, we find that the new method reaches the statistical precision on γ of an unbinned model-dependent fit, i.e. as good as possible and better than the widely used model-independent binned approach, without suffering from biases induced by a mis-modeled D decay amplitude.

Keywords: CKM Parameters, CP Violation, Bottom Quarks, Charm Flavour Violation

ArXiv ePrint: 2305.10787

https://doi.org/10.1007/JHEP09(2023)007

JHEP09(2023)007

Contents

JHEP09(2023)007

1 Introduction

The precision measurement of the CP violating phase γ (ϕ_3) is one of the primary goals of flavour physics today. The measurement of γ in $B^{\pm} \to DK^{\pm}$ and related decays [1–6] has negligible theoretical uncertainty [7]. The current precision on γ is dominated by LHCb, which measures $\gamma = \left(63.8^{+3.5}_{-3.7}\right)^{\circ}$ [8, 9]. The vast, clean datasets expected from the recently commissioned LHCb upgrade [10] and Belle II [11] will allow a sub 1° precision on γ, LHCb upgrade II is expected to reduce this further to 0.35° [12, 13]. The parameter γ is therefore set to become the most precisely measured parameter in the Cabibbo-Kobayashi-Maskawa (CKM) description of CP violation in the quark sector [14, 15], giving it a pivotal role in the search for new physics by over-constraining the Standard Model with precision measurements. To fully benefit from this potential, it is critical to control systematic uncertainties.

The measurement of γ in $B^- \to DK^-$ and its CP conjugate is possible because the neutral D meson in this decay is a superposition of D^0 and $\overline{D}^0$ that depends on γ: $D \propto D^0 + r_B e^{i(\delta_B - \gamma)} \overline{D}^0$, where $r_B \sim 0.1$ and δ_B is a CP-conserving phase induced by the

strong interaction. The neutral D meson is reconstructed in a final state accessible to both D^0 and $\overline{D}^0$. For multibody decays of the D, such as $K^0_S\pi^+\pi^-$, the CP-violating phase γ is obtained from analysing the amplitude structure of the D decay in both $B^- \to DK^-$ and $B^+ \to DK^+$ transitions; this approach is known as the BPGGSZ method [3–5].

In order to measure γ in this way, the phase difference between the D^0 and $\overline{D}^0$ decay amplitude across the Dalitz plot needs to be known. While this information can be obtained from amplitude models, these models have well-known shortcomings that make the phase information they provide unreliable, leading to significant, difficult-to-quantify systematic uncertainties. For this reason, model-independent methods are required to achieve the ultimate precision on γ. Similar considerations apply to measurements of D-mixing [16].

Model-independent methods currently in use rely on integrating over all or parts (bins) of the multibody phase space of the D decay [4, 17–21]. Two unbinned model-independent methods have been proposed recently. The method described in [22] is based on projecting the two-dimensional Dalitz plot down to one dimension, where the phase difference between the D^0 and $\overline{D}^0$ amplitudes is parameterised as a Fourier series. The authors of [23] extract γ from set of cumulative functions defined across the Dalitz plot in a way that is inspired by the Kolmogorov-Smirnov test. This method is independent of the phase difference between the D^0 and $\overline{D}^0$ amplitudes.

In all cases, one can expect some information loss due to the integration or projection process involved. Here we present a new unbinned model-independent method that optimally uses the full information across the two-dimensional Dalitz plot of a three-body decay of the neutral D meson. Using the example of $D^0 \to K^0_S\pi^+\pi^-$, we will show that this method has, with current and plausible future data sample sizes, the potential to reach essentially the same statistical precision on γ as a model-dependent method, without suffering from the associated model uncertainty.

This paper is organised as follows: in section 2 we remind the reader of the formalism for the measurement of γ in $B^\pm \to DK^\pm$ decays, and use this opportunity to introduce our notation and phase convention. Section 3 describes the new quasi model-independent method introduced in this paper. In section 4, we evaluate the performance of the new method in simulation studies for the measurement of γ in $B^\pm \to DK^\pm, D \to K^0_S\pi^+\pi^-$ decays. Finally, in section 5, we conclude.

2 Formalism

In this section we outline the formalism for the measurement of γ and the use of charm threshold data developed in [1–6], to remind the reader and fix the notation. For simplicity, we ignore the effects of D mixing [24–27]. In most cases, these effects are small enough to be negligible [26]. Where they are not, they can be taken into account as described in [27].

2.1 Notation and conventions

We use the notation $A^f_D(\mathbf{p})$ for the decay amplitude of the D^0 meson to a final state f, at point $\mathbf{p}$ in the $D \to f$ Dalitz plot and $\overline{A}^f_D(\overline{\mathbf{p}})$ for that of the CP-conjugate process.

JHEP09(2023)007

Our phase convention for the CP operator is such that $CP|D^0\rangle = |\overline{D}^0\rangle$, which is the usual practice in the context of beauty decays to charm. An alternative convention where $CP|D^0\rangle = -|\overline{D}^0\rangle$ is widely used in the context of charm physics.

With our phase convention, and assuming the absence of CP violation in charm decays, $A_D^f(\mathbf{p}) = \overline{A}_D^f(\overline{\mathbf{p}})$. For self-conjugate final states such as $K_S^0\pi^+\pi^-$, which we will use for the simulation studies presented below, $\mathbf{p}$ and $\overline{\mathbf{p}}$ are in the same Dalitz plot. We parameterise the $D^0 \to K_S^0\pi^+\pi^-$ Dalitz plot with the usual variables $s_+ = m^2(K_S^0\pi^+)$ and $s_- = m^2(K_S^0\pi^-)$, representing the invariant mass-squared of the $K_S^0\pi^+$ and $K_S^0\pi^-$ pair, respectively. If $\mathbf{p} = (s_-, s_+)$, then $\overline{\mathbf{p}} = (s_+, s_-)$, and $\overline{A}_D^{K_S^0\pi\pi}(s_+, s_-) = A_D^{K_S^0\pi\pi}(s_-, s_+)$.

We define the phases $\phi_D^f(\mathbf{p}) \equiv \arg(A_D^f(\mathbf{p})), \overline{\phi}_D^f(\mathbf{p}) \equiv \arg(\overline{A}_D^f(\mathbf{p}))$ and the phase difference $\delta_D^f(\mathbf{p}) \equiv \phi_D^f(\mathbf{p}) - \overline{\phi}_D^f(\mathbf{p})$. It is also useful to define $\overline{\delta}_D^f(\mathbf{p}) \equiv \overline{\phi}_D^f(\mathbf{p}) - \phi_D^f(\mathbf{p})$, even though it is trivially related to δ_D through $\overline{\delta}_D^f(\mathbf{p}) = \delta_D^f(\overline{\mathbf{p}}) = -\delta_D^f(\mathbf{p})$. To declutter the notation we will omit the superscripts and/or the $(\mathbf{p})$, where there is no risk of ambiguity.

When applying the method presented below in practice it will frequently be necessary to combine results obtained using different conventions for the phase of the CP operator. Switching from our convention with $CP|D^0\rangle = |\overline{D}^0\rangle$ to the convention with $CP|D^0\rangle = -|\overline{D}^0\rangle$ corresponds to the change $\delta_D \to \delta_D + \pi$.

2.2 Measuring γ with $B^\pm \to DK^\pm$ decays

The decay amplitude of a D meson resulting from a $B^- \to DK$ to a final state f at phase space point $\mathbf{p}$ is given by

$$A_{B-}(\mathbf{p}) \propto A_D(\mathbf{p}) + r_B e^{i(\delta_B - \gamma)} \overline{A}_D(\mathbf{p}), \tag{2.1}$$

and the corresponding decay rate is

$$\begin{aligned}
\Gamma^-(\mathbf{p}) &= N\left(|A_D(\mathbf{p})|^2 + r_B^2|\overline{A}_D(\mathbf{p})|^2 + 2\mathsf{Re}(A_D(\mathbf{p}) r_B e^{-i(\delta_B(\mathbf{p}) - \gamma)} \overline{A}_D^*(\mathbf{p}))\right) && (2.2)\\
&= N\left(|A_D(\mathbf{p})|^2 + r_B^2|\overline{A}_D(\mathbf{p})|^2 + 2r_B|A_D(\mathbf{p})||\overline{A}_D(\mathbf{p})|\cos(-\delta_B + \gamma + \delta_D)\right) && (2.3)\\
&= N(|A_D(\mathbf{p})|^2 + r_B^2|\overline{A}_D(\mathbf{p})|^2 \\
&\quad + 2r_B|A_D(\mathbf{p})||\overline{A}_D(\mathbf{p})|\left(\cos(\delta_B - \gamma)\cos(\delta_D(\mathbf{p})) + \sin(\delta_B - \gamma)\sin(\delta_D(\mathbf{p}))\right)), && (2.4)
\end{aligned}$$

where N is a normalisation factor. For the CP-conjugate process, with a D from a $B^+ \to DK^+$:

$$\begin{aligned}
\Gamma^+(\overline{\mathbf{p}}) &= N(|\overline{A}_D(\overline{\mathbf{p}})|^2 + r_B^2|A_D(\overline{\mathbf{p}})|^2 \\
&\quad + 2r_B|A_D(\overline{\mathbf{p}})||\overline{A}_D(\overline{\mathbf{p}})|\left(\cos(\delta_B + \gamma)\cos(\overline{\delta}_D) + \sin(\delta_B + \gamma)\sin(\overline{\delta}_D(\overline{\mathbf{p}}))\right)) && (2.5)
\end{aligned}$$

where $\overline{A}_D(\overline{\mathbf{p}}) = A_D(\mathbf{p})$, $A_D(\overline{\mathbf{p}}) = \overline{A}_D(\mathbf{p})$, and $\overline{\delta}_D(\overline{\mathbf{p}}) = \delta_D(\mathbf{p})$ for CP conservation in charm. For the fits in our validation studies, we follow the widely used practice to re-parameterise the decay rates in terms of the "cartesian" variables

$$x_+ \equiv r_B\cos(\delta_B + \gamma), \quad y_+ \equiv r_B\sin(\delta_B + \gamma), \quad x_- \equiv r_B\cos(\delta_B - \gamma), \quad y_- \equiv r_B\sin(\delta_B - \gamma). \tag{2.6}$$

JHEP09(2023)007

This is motivated by the observation that fits in terms of $x_\pm$ and $y_\pm$ are statistically better behaved than those in terms of r_B, δ_B, and γ, which is related to the fact that there is no sensitivity to δ_B, γ as $r_B \to 0$. The decay rates in terms of the new variables are

$$\Gamma^-(\mathbf{p}) = N\left(|A_D|^2 + \left(x_-^2 + y_-^2\right)|\overline{A}_D|^2 + 2|A_D||\overline{A}_D|\left(x_- \cos(\delta_D) + y_- \sin(\delta_D)\right)\right), \quad (2.7)$$

$$\Gamma^+(\overline{\mathbf{p}}) = N\left(|\overline{A}_D|^2 + \left(x_+^2 + y_+^2\right)|A_D|^2 + 2|A_D||\overline{A}_D|\left(x_+ \cos(\overline{\delta}_D) + y_+ \sin(\overline{\delta}_D)\right)\right). \quad (2.8)$$

In a model-dependent approach, A_D and $\overline{A}_D$ are derived from a high-statistics amplitude fit to flavour-specific D^0, $\overline{D}^0$ decays. However, the models used to describe the decay amplitude have theoretical shortcomings that make their phase information, which enters via δ_D, unreliable. This in turn translates into a systematic uncertainty on γ.

For the model-independent approach described in [4, 18], one integrates over regions (bins) of phase space. These bins are defined such that they form *CP*-conjugate pairs and we label them such that the *CP*-conjugate of bin i is bin $-i$. In what follows, we assume the D decays to $K^0_S\pi^+\pi^-$, although the approach clearly generalises to other decay modes. We define the following parameters related to $|A_D|^2, |\overline{A}_D|^2$:

$$F_i \equiv \int_{\text{bin } i} |A_D|^2 ds_+ ds_-, \qquad \overline{F}_i \equiv \int_{\text{bin } i} |\overline{A}_D|^2 ds_+ ds_-. \quad (2.9)$$

In the absence of *CP* violation in charm, $\overline{F}_i = F_{-i}$. We also define the following parameters related to the phase-difference between A_D and $\overline{A}_D$:

$$c_i \equiv \frac{\int_{\text{bin } i} |A_D||\overline{A}_D| \cos(\delta_D) ds_+ ds_-}{\sqrt{\int_{\text{bin } i} |A_D|^2 ds_+ ds_- \int_{\text{bin } i} |\overline{A}_D|^2 ds_+ ds_-}}, \quad (2.10)$$

$$s_i \equiv \frac{\int_{\text{bin i}} |A_D||\overline{A}_D| \sin(\delta_D) ds_+ ds_-}{\sqrt{\int_{\text{bin i}} |A_D|^2 ds_+ ds_- \int_{\text{bin i}} |\overline{A}_D|^2 ds_+ ds_-}}, \quad (2.11)$$

which implies $c_{-i} \equiv c_i$ and $s_{-i} \equiv -s_i$. In terms if these quantities, the decay rate $B^- \to DK^-$ with the D decay in phase-space bin i, is given by

$$\Gamma_i^- = F_i + r_B^2 F_{-i} + 2r_B\sqrt{F_i F_{-i}}\left(\cos(\delta_B - \gamma)c_i + \sin(\delta_B - \gamma)s_i\right). \quad (2.12)$$

The *CP* conjugate process, a $B^+ \to DK^+$ decay with the D decay in phase-space bin $-i$, is

$$\Gamma_{-i}^+ = F_i + r_B^2 F_{-i} + 2r_B\sqrt{F_i F_{-i}}\left(\cos(\delta_B + \gamma)c_i + \sin(\delta_B + \gamma)s_i\right). \quad (2.13)$$

Equivalently, these decay rates can be expressed in terms of $x_\pm, y_\pm$:

$$\Gamma_i^- = F_i + \left(x_-^2 + y_-^2\right)F_{-i} + 2\sqrt{F_i F_{-i}}\left(x_- c_i + y_- s_i\right), \quad (2.14)$$

$$\Gamma_{-i}^+ = F_i + \left(x_+^2 + y_+^2\right)F_{-i} + 2\sqrt{F_i F_{-i}}\left(x_+ c_i + y_+ s_i\right). \quad (2.15)$$

All parameters related to the charm decay, i.e. F_i, c_i, and s_i, can be directly obtained from data, where data from the charm threshold are critical to constraining the parameters related to the phase difference of A_D and $\overline{A}_D$, i.e. c_i and s_i. It is worth noting, though, that

JHEP09(2023)007

the c_i and s_i can be obtained alongside γ from (a sufficiently large sample of) $B^\pm \to DK^\pm$ decays [4]; however, the input from the charm threshold dramatically improves the fit. Measurements of γ in this way, using the $D \to K^0_S\pi^+\pi^-$ Dalitz plot we focus on here, have been made by Belle [28, 29], Belle & Belle II [30], and LHCb [31–33], using input from CLEO-c [34, 35] and BES III [36, 37]. We will below introduce a new method, also based on exploiting threshold data, that does not require binning, or other forms of integration over phase space as in [22, 23]. This is motivated by the aim to maximise the use of information contained in the full two-dimensional Dalitz plot.

2.3 Charm threshold data

At the charm threshold, $\psi(3770)$ are produced and decay approximately 50% of the time to a pair of neutral D mesons that we label D_1, D_2. The resulting system of D mesons must be C-odd, like the $\psi(3770)$ they originate from. Therefore:

$$|\psi(3770)\rangle \to |D^0\rangle_1|\overline{D}^0\rangle_2 - |\overline{D}^0\rangle_1|D^0\rangle_2. \tag{2.16}$$

Let D_1 decay to final state f at phase-space point $\mathbf{p}$ and D_2 to final state g at phase-space point $\mathbf{q}$. Then the decay amplitude for this process is

$$A(\psi \to D_1D_2; D_1 \to f(\mathbf{p}), D_2 \to g(\mathbf{q})) = \frac{1}{\sqrt{2}}\left(A^f_D(\mathbf{p})\overline{A}^g_D(\mathbf{q}) - \overline{A}^f_D(\mathbf{p})A^g_D(\mathbf{q})\right). \tag{2.17}$$

We will call g the *tag* and f the *signal* (in our feasibility study, f will be $K^0_S\pi^+\pi^-$). Depending on the tag, we can distinguish a few important special cases:

1. $D_2 \to g$ is a flavour-specific decay such as a semileptonic decay, or a quasi-flavour-specific decay such as $D^0 \to K^-\pi^+$ (in our feasibility studies, we will ignore the small dilution effect due to the suppressed decay $\overline{D}^0 \to K^-\pi^+$, although this can be taken into account). Then

$$A(\psi \to D_1D^0; D_1 \to f(\mathbf{p}), D^0 \to g) \propto \overline{A}^f_D(\mathbf{p}), \tag{2.18}$$

and similarly

$$A(\psi \to D_1\overline{D}^0; D_1 \to f(\mathbf{p}), \overline{D}^0 \to g) \propto A^f_D(\mathbf{p}). \tag{2.19}$$

We refer to these decays as flavour tagged. They provide the same information as flavour-tagged D^0 decays at the B-factories and LHCb, where the flavour is usually identified through the charge of the pion in $D^{*+} \to D^0\pi^+$ and $D^{*-} \to \overline{D}^0\pi^-$ decays. Measurements of flavour-tagged decays provide $|A_D(\mathbf{p})|$ and, in the binned approach, F_i. (In recent LHCb analyses, though, F_i, and associated efficiency effects, have been obtained from simultaneous fits to $B^\pm \to DK^\pm$ and $B^\pm \to D\pi^\pm$ data [33, 38].)

2. $D_2 \to g$ is a CP-specific decay, either a CP-even decay such as $D_2 \to K^+K^-$, implying $|D_2\rangle = \frac{1}{\sqrt{2}}\left(|D^0\rangle + |\overline{D}^0\rangle\right) =: D_+$, or CP-odd such as $D_2 \to K^0_S\pi^0$, implying $|D_2\rangle = \frac{1}{\sqrt{2}}\left(|D^0\rangle - |\overline{D}^0\rangle\right) =: D_-$, where the expressions for the superpositions of D^0

JHEP09(2023)007

and $\overline{D}^0$ are convention-dependent; we use a convention where $CP|D^0\rangle = |\overline{D}^0\rangle$. The corresponding decay amplitudes are

$$A(\psi \to D_1 D_\pm; D_1 \to f(\mathbf{p}), D_\pm \to g) \propto \mp A_D^f(\mathbf{p}) - \overline{A}_D^f(\mathbf{p}), \tag{2.20}$$

and the decay rates:

$$\begin{aligned}\Gamma(&\psi \to D_1 D_\pm; D_1 \to f(\mathbf{p}), D_2 \to g) \\ &\propto |A_D^f(\mathbf{p})|^2 + |\overline{A}_D^f(\mathbf{p})|^2 \pm 2|A_D^f(\mathbf{p})||\overline{A}_D^f(\mathbf{p})| \cos(\delta_D(\mathbf{p})).\end{aligned} \tag{2.21}$$

These provide information on $\cos(\delta_D)$, or, in the binned approach, c_i.

3. Both D mesons decay to the same self-conjugate signal mode e.g. $K_S^0\pi^+\pi^-$:

$$A(\psi \to D_1 D_2; D_1 \to f(\mathbf{p}), D_2 \to f(\mathbf{q})) \propto A_D(\mathbf{p})\overline{A}_D(\mathbf{q}) - \overline{A}_D(\mathbf{p})A_D(\mathbf{q}), \tag{2.22}$$

with a decay rate

$$\begin{aligned}\Gamma(&\psi \to D_1 D_2; D_1 \to f(\mathbf{p}), D_2 \to f(\mathbf{q})) \\ &\propto |A_D(\mathbf{p})|^2|\overline{A}_D(\mathbf{q})|^2 + |\overline{A}_D(\mathbf{p})|^2|A_D(\mathbf{q})|^2 \\ &\quad - 2|A_D(\mathbf{p})||\overline{A}_D(\mathbf{q})||\overline{A}_D(\mathbf{p})||A_D(\mathbf{q})| \cos(\delta_D(\mathbf{p}) - \delta_D(\mathbf{q}))\end{aligned} \tag{2.23}$$

$$\begin{aligned}&\propto |A_D(\mathbf{p})|^2|\overline{A}_D(\mathbf{q})|^2 + |\overline{A}_D(\mathbf{p})|^2|A_D(\mathbf{q})|^2 \\ &\quad - 2|A_D(\mathbf{p})||\overline{A}_D(\mathbf{q})||\overline{A}_D(\mathbf{p})||A_D(\mathbf{q})| \\ &\quad\quad \times (\cos(\delta_D(\mathbf{p}))\cos(\delta_D(\mathbf{q})) + \sin(\delta_D(\mathbf{p}))\sin(\delta_D(\mathbf{q}))) .\end{aligned} \tag{2.24}$$

This category is therefore sensitive to both $\sin(\delta_D)$ and $\cos(\delta_D)$, in contrast to CP-tagged decays which are only sensitive to $\cos(\delta_D)$. In the binned approach, this translates into unique sensitivity to s_i.

Measurements of c_i and s_i for $D \to K_S^0\pi^+\pi^-$ have been made at CLEO-c [34, 35] and more recently BES III [36, 37].

3 Quasi model independent unbinned method to measure γ

3.1 Basic idea

This section will introduce the quasi model-independent (QMI) method that is the subject of this paper. For concreteness, we will consider the decay $D^0 \to K_S^0\pi^+\pi^-$, although the method generalises to all self-conjugate charm decays, and with some modification also to non-self-conjugate ones.

The statistically most precise way of measuring γ is the model-dependent method. We observe that the magnitude of the amplitude structure across the Dalitz plot of $D^0 \to K_S^0\pi^+\pi^-$ is well known from flavour-specific D^0 and $\overline{D}^0$ decays analysed by BaBar and Belle [39]. The D^0, $\overline{D}^0$ datasets used in these fits are orders of magnitude larger than the $B^\pm \to DK^\pm$ datasets available for γ measurements. The fact that the collaborations achieve a decent fit of their models to these datasets implies that we can trust the magnitude

JHEP09(2023)007

of existing amplitude models. However, those models violate unitarity and analyticity, which breaks the connection between magnitude and phase. Consequently, the phases of these models stand on less firm ground. Our approach is therefore to correct the model's phase in a model-independent way, or, more precisely, correct the *phase difference* between the D^0 amplitude $A_D(\mathbf{p})$ and $\overline{D}^0$ amplitude $\overline{A}_D(\mathbf{p})$ at each phase space point $\mathbf{p}$. These phase differences are all that matters and in fact it is all we have access to. Measurements of c_i and s_i by CLEO-c and BES III suggest that the model's phase differences are at least approximately correct [34–37]. Our approach is therefore to obtain the model-independent phase difference by adding a correcting term δ_D^{corr} to the model's phase difference δ_D^{model},

$$\delta_D = \delta_D^{\text{model}} + \delta_D^{\text{corr}}. \tag{3.1}$$

We parameterise δ_D^{corr} in a generic way, as a power series in the Dalitz plot parameters. We assume CP conservation in charm decays, such that

$$\delta_D(s_+, s_-) = -\delta_D(s_-, s_+), \tag{3.2}$$

which also implies

$$\delta_D^{\text{corr}}(s_+, s_-) = -\delta_D^{\text{corr}}(s_-, s_+). \tag{3.3}$$

This symmetry reduces the number of parameters needed to parameterise δ_D^{corr}. We will see below that even if we depart from the assumption that the model's phase differences are approximately correct, such that δ_D^{corr} becomes quite sizeable, our method still works.

The information that allows us to constrain δ_D^{corr} comes, as for the binned methods, predominantly from the charm threshold, although $B^\pm \to DK^\pm$ decays also contribute.

3.2 Constructing the correction to δ_D

In order to implement the symmetry relation eq. (3.3), we define the variables

$$z_+ \equiv s_+ + s_-, \qquad z_- \equiv s_+ - s_-. \tag{3.4}$$

Now the symmetry condition from eq. (3.3) becomes $\delta_D^{\text{corr}}(z_+, z_-) = -\delta_D^{\text{corr}}(z_+, -z_-)$ and can be implemented by only allowing terms with odd powers of z_- in the correcting polynomial.

We found that parameterising the phase in terms of Legendre polynomials works well. These are defined for values $x \in [-1, 1]$. We therefore scale z_+, z_-

$$z'_+ = \frac{2z_+ - (z_+^{\max} + z_+^{\min})}{z_+^{\max} - z_+^{\min}}, \qquad z'_- = \frac{2z_- - (z_-^{\max} + z_-^{\min})}{z_-^{\max} - z_-^{\min}}, \tag{3.5}$$

where the superscripts max and min indicate the maximum and minimum values of the unprimed parameters. The kinematically allowed region of the $K^0_S\pi^+\pi^-$ in terms of the normalised, rotated parameters z'_+, z'_- is shown in figure 1b. The figure shows that within the square $z'_+ \in [-1, 1], z'_- \in [-1, 1]$ where the Legendre polynomial is defined, there is a lot of space where there are no data, with the kinematically-allowed interval in z'_- varying a lot as a function of z_+. We therefore "stretch" the Dalitz plot by replacing z'_- with

$$z''_- = \frac{2z'_-}{z'_+ + 2}. \tag{3.6}$$

JHEP09(2023)007

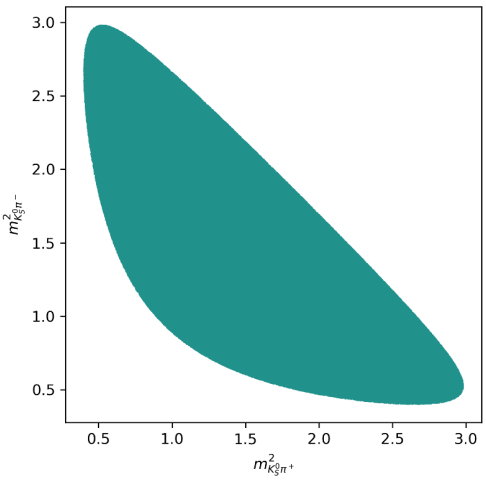

(a) Dalitz Phasepace in terms of s_+, s_-.

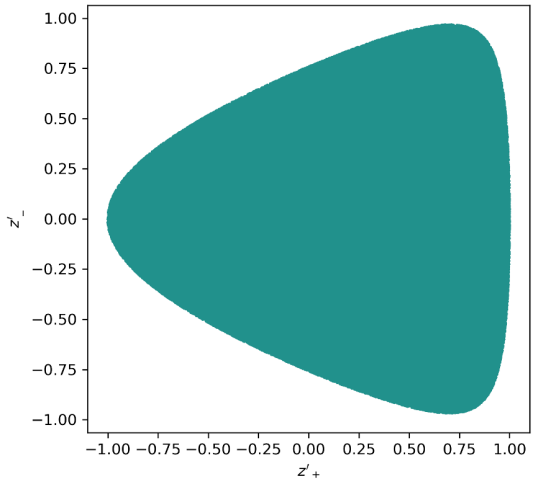

(b) Rotated Dalitz Phasepace.

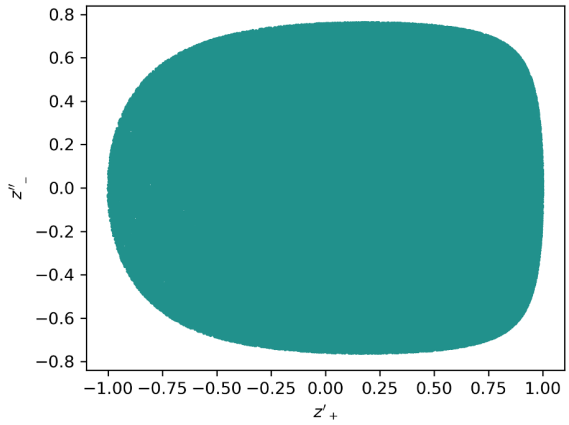

(c) Stretched Rotated Dalitz Phasepace.

Figure 1. The Dalitz Phasespace, (s_+, s_-), shaped to the rotated coordinates, (z'_+, z'_-) and the stretched rotated coordinates, (z'_+, z''_-).

The Dalitz plot phase space for the different parametrisations is shown in figure 1. Alternatives such as a variation of the square Dalitz plot [40] would have achieved a similar outcome.

We construct the correcting polynomial, δ_D^{corr}, of order N with free parameters $\mathbf{C}$

$$\delta_D^{\text{corr}}(z'_+, z''_-|\mathbf{C}) = \sum_{i=0}^{i\leq N} \sum_{j=0}^{j\leq \frac{N-i}{2}} C_{i,2j+1} P_i(z'_+) P_{2j+1}(z''_-), \tag{3.7}$$

where P_n are, in our implementation, n^{th} order Legendre polynomials, although any function with $P_{2j+1}(z''_-) = -P_{2j+1}(-z''_-)$ would be equally valid. The coefficients C_{ij} are free parameters, determined together with $x_\pm, y_\pm$ in a simultaneous fit to $\psi(3770)$ and $B^\pm \to DK^\pm$ data.

JHEP09(2023)007

Tag (g)	Events
CP-even, e.g. $D \to K^+K^-$	2546
CP-odd, e.g. $D \to K^0_S\pi^0$	1725
D^0 flavour, e.g. $D^0 \to K^-\pi^+$	23457
$\overline{D}^0$ flavour, e.g. $\bar{D}^0 \to K^+\pi^-$	23457
$D \to K^0_S\pi^+\pi^-$ (double tag)	1833

Table 1. $\psi(3770) \to D_1D_2, D_1 \to K^0_S\pi^+\pi^-, D_2 \to g$, decays generated for our simulation studies. D_1, D_2 represent superpositions of D^0 and $\overline{D}^0$, depending on the tag. CP even (odd) tags imply CP-odd (even) $D \to K^0_S\pi^+\pi^-$ decays and D^0 ($\overline{D}^0$) flavour tags imply $\overline{D}^0$ (D^0) decays to $K^0_S\pi^+\pi^-$. Sample sizes are taken from [37].

4 Simulation studies

We test the algorithm in simulation studies where we generate charm threshold and $B^\pm \to DK^\pm$ data according to the equations given in section 2.2 and 2.3, using the $D^0 \to K^0_S\pi^+\pi^-$ model in `AmpGen` [41]. We ignore backgrounds and efficiency effects in this study.

Using a modified version of AmpGen, we also generate data where we apply a change to the phase of the decay amplitude relative to the model assumed in the fit. We will then show how our new unbinned approach removes the bias this would inflict on the fitted value of γ in a model-dependent approach, and how it does so with improved statistical uncertainty compared to the binned method.

4.1 Simulated data

4.1.1 Sample sizes

In our default settings, we simulate charm threshold data according to the event numbers given in BES III's latest $D \to K^0_S\pi^+\pi^-$ analysis [37] and $B^\pm \to DK^\pm, D \to K^0_S\pi^+\pi^-$ event yields reported in LHCb's latest measurement of γ in this decay mode [33]. The BES III signal yields for the different tags are shown in table 1. For the purpose of this study, we treat $D^0 \to K^-\pi^+$ and $\overline{D}^0 \to K^+\pi^-$ as pure flavour tags and ignore the small contributions from $\overline{D}^0 \to K^-\pi^+$ and $D^0 \to K^+\pi^-$. LHCb report a total of $12,533$ $B^\pm \to DK^\pm, D \to K^0_S\pi^+\pi^-$ decays. We split this evenly between $B^- \to DK^-$ and $B^+ \to DK^+$, and generate on average 6267 events for each. This implies that, as in LHCb's analysis, our fits are entirely based on the distribution of events within each Dalitz plot, not $B^+ \to DK^+$ and $B^- \to DK^-$ event yields integrated across the whole Dalitz plot. We also consider scenarios with larger datasets - by a factor of 100 for $B^\pm \to DK^\pm, D \to K^0_S\pi^+\pi^-$ and by a factor of 10 for charm threshold data.

4.1.2 Amplitudes with modified phases

We generate events based on the nominal amplitude model from BaBar and Belle's joint analysis [39], but with a modified phase difference

$$\delta_D^{\text{model}}(\mathbf{p}) \to \delta_D^{\text{model}}(\mathbf{p}) + f(\mathbf{p}) \tag{4.1}$$

JHEP09(2023)007

	A	ε	μ_+	σ_+	μ_-	σ_-
f_{single}	1	0.1	2.0	0.75	0.90	0.25
f_{double} subscript 1	1	0.1	1.0	0.25	1.25	1.0
f_{double} subscript 2	-1	0.1	2.5	0.25	1.25	1.0

Table 2. Parameters used for scenarios two (f_{single}) and three (f_{double}), where for f_{double} the top row refers to the parameters with subscript 1 in eq. (4.4), and the bottom row refers those with subscript 2. The parameters ε, μ and σ are given in units of $\left(\text{GeV}/c^2\right)^2$.

Note that the expressions for decay rates (2.4), (2.5), (2.7), (2.8), (2.21), (2.24) only depend on the phase differences between A_D and $\overline{A}_D$, never the absolute phases of A_D or $\overline{A}_D$ themselves. The function $f(\mathbf{p})$ modifies this phase difference. Our approach assures that the magnitudes $|A_D|, |\overline{A}_D|$ remain unchanged. We generate events according to three scenarios:

1. no phase modification, $f_0 = 0$,

2. single Gaussian modification

$$f_{\text{single}}(s_+, s_-|A, \varepsilon, \mu_+, \mu_-, \sigma_+, \sigma_-) = A \text{ erf}\left(\frac{s_+ - s_-}{\varepsilon}\right) e^{-G(s_+,s_-|\mu_\pm,\sigma_\pm)}, \tag{4.2}$$

   with

$$G\left(s_+, s_-\right) = \begin{cases} \frac{(s_+-\mu_+)^2}{\sigma_+^2} + \frac{(s_--\mu_-)^2}{\sigma_-^2} & s_+ > s_-, \\ \frac{(s_--\mu_+)^2}{\sigma_+^2} + \frac{(s_+-\mu_-)^2}{\sigma_-^2} & s_+ < s_-, \end{cases} \tag{4.3}$$

3. double Gaussian modification

$$\begin{aligned} f_{\text{double}}(s_+, s_-) = f_{\text{single}}(s_+, s_-|A_1, \varepsilon_1, \mu_{+1}, \mu_{-1}, \sigma_{+1}, \sigma_{-1}) \\ + f_{\text{single}}(s_+, s_-|A_2, \varepsilon_2, \mu_{+2}, \mu_{-2}, \sigma_{+2}, \sigma_{-2}). \end{aligned} \tag{4.4}$$

The purpose of the error function, $\text{erf(x)} \equiv \frac{2}{\sqrt{\pi}} \int_0^x e^{-t^2}\, dt$, in the definition of f_{single} is to implement the condition $f(s_+, s_-) = -f(s_-, s_+)$ while providing a smooth transition across the line $s_+ = s_-$. The parameter values used for scenarios two and three are given in table 2. The phase modifications they induce are shown in figure 2, which shows f_{single} and f_{double}, in radians. It can be seen that scenario two targets the region of the K^* resonance, while scenario three has large phase modifications especially in the region of the $\rho K_S^0 - K^*\pi$ interference. It is worth noting that the phase change relative to the nominal model we consider here is up to ± 1 radian, which is not a small shift.

4.1.3 Other input parameters

All samples are generated with the 2022 HFLAV [42] averages $r_B = 0.093, \delta_B = 119.5°, \gamma = 69.5°$, which corresponds to

$$x_+ = -0.09186, \qquad y_+ = -0.01455; \qquad x_- = 0.05978, \qquad y_- = 0.07124. \tag{4.5}$$

JHEP09(2023)007

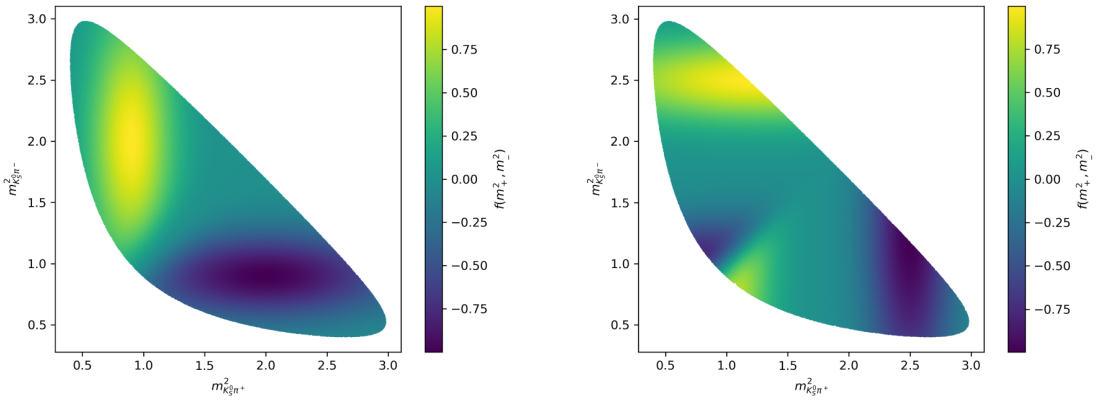

(a) Single peak bias.

(b) Double peak bias.

Figure 2. The figures show the difference between the phase difference $\delta_D(s_+, s_-)$ of the nominal amplitude model and the model with which the data are actually generated, for the two biased scenarios considered.

4.2 Fit results

4.2.1 Order by order fits to individual samples

We perform fits with the model-dependent (MD) method and with the quasi model-independent (QMI) method with phase-correction polynomials of order $N = 1, 2, \ldots, 9$, for one sample of each of the phase-modification scenarios. Beyond $N = 9$, fits converge very slowly due to the large number of parameters. The results are shown in tables 3, 4, and 5, in the format (fit result) − (input value) ± (uncertainty), in units of 10^{-2}; the uncertainty is that estimated by the MINUIT2 [43]-based AmpGen [41] fitter (validated below, in section 4.2.2). We see in table 3, where there is no phase modification relative to the nominal amplitude model, that the model-dependent and the quasi-model-independent fit both reproduce the input values, within uncertainties. For correction polynomials of order $N > 3$, the fit results differ slightly between the methods, but far less than the statistical uncertainty. The validation studies below show that this does not lead to a systematic bias. Tables 4 and 5 show that the phase modifications induce a significant bias in $x_\pm, y_\pm$ in the model-dependent method, and how the QMI method recovers from it. The changes in the fit results for $x_\pm, y_\pm$ between the model-dependent and the higher order QMI fits correspond to changes in the estimated values of r_B, δ_B, and γ of 0.006, 11°, and 7° for the double-Gaussian bias (table 5), and of 0.021, 23°, and 0.3° for the single-Gaussian bias (table 4). An interesting feature is that the uncertainties on $x_\pm$ and $y_\pm$ do not appear to be affected significantly by the additional fit parameters. This conclusion is confirmed in the validation studies shown below.

4.2.2 Fits to 100 pseudoexperiments

We generate 100 pseudoexperiments and fit them with the model-dependent method, the binned method, and the QMI method. The QMI method uses a 6^{th} order correction polynomial. Table 6 shows the mean and standard deviation of the distribution of residuals

JHEP09(2023)007

Order	$\Delta x_+ \cdot 100$	$\Delta y_+ \cdot 100$	$\Delta x_- \cdot 100$	$\Delta y_- \cdot 100$
MD	-0.9 ± 0.8	-1.1 ± 1.1	-1.5 ± 0.9	$+1.0 \pm 0.9$
1	-0.9 ± 0.8	-1.0 ± 1.1	-1.5 ± 0.9	$+0.9 \pm 0.9$
2	-0.9 ± 0.8	-1.0 ± 1.1	-1.5 ± 0.9	$+1.0 \pm 0.9$
3	-0.9 ± 0.8	-1.2 ± 1.1	-1.5 ± 0.9	$+1.1 \pm 0.9$
4	-0.8 ± 0.8	-1.1 ± 1.1	-1.6 ± 0.9	$+1.2 \pm 0.9$
5	-0.9 ± 0.8	-1.1 ± 1.1	-1.6 ± 0.9	$+1.2 \pm 0.9$
6	-0.9 ± 0.8	-1.1 ± 1.2	-1.5 ± 0.9	$+1.1 \pm 0.9$
7	-0.9 ± 0.8	-1.1 ± 1.2	-1.5 ± 0.9	$+1.1 \pm 0.9$
8	-0.8 ± 0.8	-1.3 ± 1.2	-1.6 ± 0.9	$+1.3 \pm 0.9$
9	-0.8 ± 0.8	-1.4 ± 1.2	-1.6 ± 0.9	$+1.3 \pm 0.9$

Table 3. Order to order fit for the unbiased δ_D sample.

Order	$\Delta x_+ \cdot 100$	$\Delta y_+ \cdot 100$	$\Delta x_- \cdot 100$	$\Delta y_- \cdot 100$
MD	-1.8 ± 0.8	$+4.0 \pm 1.1$	$+1.0 \pm 0.9$	-3.7 ± 0.9
1	-0.6 ± 0.8	$+1.0 \pm 1.0$	$+1.4 \pm 0.9$	-0.8 ± 0.9
2	-0.7 ± 0.8	$+0.9 \pm 1.0$	$+1.4 \pm 0.9$	-0.7 ± 0.9
3	-0.3 ± 0.8	$+0.3 \pm 1.1$	$+1.1 \pm 0.9$	$+0.5 \pm 1.0$
4	-0.3 ± 0.8	$+0.2 \pm 1.0$	$+1.1 \pm 0.9$	$+0.7 \pm 1.0$
5	-0.2 ± 0.8	$+0.1 \pm 1.1$	$+1.1 \pm 0.9$	$+0.9 \pm 1.0$
6	-0.2 ± 0.8	-0.1 ± 1.0	$+1.0 \pm 0.9$	$+0.9 \pm 1.0$
7	-0.2 ± 0.8	-0.2 ± 1.0	$+1.0 \pm 0.9$	$+1.0 \pm 1.0$
8	-0.2 ± 0.8	-0.3 ± 1.0	$+1.1 \pm 0.9$	$+0.9 \pm 1.0$
9	-0.2 ± 0.8	-0.2 ± 1.0	$+1.1 \pm 0.9$	$+0.9 \pm 1.0$

Table 4. Order to order fit for $\delta_D + f_{\text{single}}(s_+, s_-)$ sample.

(i.e. fit result minus truth value) for these fits. Table 7 shows the corresponding value for the pull, which is the residual divided by the uncertainty reported by the fit. The results show that, in the absence of any phase modification, the model-dependent and the QMI method both yield unbiased results with essentially the same uncertainty. The pulls for the QMI method, and for the unbiased data also those for the model-dependent method, show generally good agreement with the expected mean of zero and standard deviation of one. For both methods, the uncertainty the fitter reports on x_+ seems to be slightly over-estimated. There appears to be a slight under-estimation of the y_- uncertainty in the f_{single} configuration. The results with the two phase modification scenarios confirm that the phase modifications induce significant biases in the fit results of the model-dependent method, while the QMI results remain unbiased.

JHEP09(2023)007

Order	$\Delta x_+ \cdot 100$	$\Delta y_+ \cdot 100$	$\Delta x_- \cdot 100$	$\Delta y_- \cdot 100$
MD	$+1.3 \pm 0.8$	$+1.2 \pm 1.1$	-1.0 ± 1.3	-3.3 ± 1.3
1	$+1.1 \pm 0.8$	$+0.5 \pm 1.0$	-1.3 ± 0.8	-0.6 ± 1.0
2	$+0.5 \pm 0.9$	$+0.1 \pm 1.0$	-1.0 ± 0.8	$+0.4 \pm 1.0$
3	$+0.6 \pm 0.8$	0.0 ± 1.0	-1.2 ± 0.8	$+0.4 \pm 1.0$
4	$+0.3 \pm 0.8$	$+0.4 \pm 1.0$	-0.8 ± 0.8	$+0.3 \pm 1.0$
5	$+0.4 \pm 0.8$	$+0.5 \pm 1.0$	-0.7 ± 0.8	$+0.3 \pm 1.0$
6	$+0.3 \pm 0.8$	$+0.7 \pm 1.0$	-0.8 ± 0.8	$+0.4 \pm 1.0$
7	$+0.3 \pm 0.8$	$+0.5 \pm 1.0$	-0.9 ± 0.8	$+0.7 \pm 1.0$
8	$+0.3 \pm 0.8$	$+0.5 \pm 1.0$	-0.9 ± 0.8	$+0.7 \pm 1.0$
9	$+0.3 \pm 0.8$	$+0.5 \pm 1.0$	-0.7 ± 0.8	$+0.7 \pm 1.0$

Table 5. Order to order fit for $\delta_D + f_{\text{double}}(s_+, s_-)$ sample.

phase mod.	Method	$(\Delta x_+ \pm \sigma_{x_+})$ $\times 100$	$(\Delta y_+ \pm \sigma_{y_+})$ $\times 100$	$(\Delta x_- \pm \sigma_{x_-})$ $\times 100$	$(\Delta y_- \pm \sigma_{y_-})$ $\times 100$
$f_0 = 0$	QMI	-0.1 ± 0.6	$+0.1 \pm 1.1$	-0.1 ± 1.0	0.0 ± 1.0
	MD	-0.1 ± 0.6	$+0.1 \pm 1.1$	-0.1 ± 0.9	-0.1 ± 1.0
f_{single}	QMI	$+0.1 \pm 0.7$	$+0.1 \pm 1.1$	$+0.4 \pm 0.9$	-0.1 ± 1.1
	MD	$+0.9 \pm 0.7$	$+3.6 \pm 1.1$	$+0.3 \pm 0.9$	-3.7 ± 1.2
f_{double}	QMI	$+0.1 \pm 0.7$	-0.0 ± 1.0	$+0.1 \pm 0.9$	$+0.2 \pm 1.0$
	MD	$+0.5 \pm 0.7$	$+1.8 \pm 1.1$	$+0.1 \pm 1.0$	-1.6 ± 1.0

Table 6. Residuals from 100 fits to samples without any phase modification, with the quasi-model-independent (QMI) and the model-dependent (MD) method. The QMI fit uses a 6th order phase-correction polynomial. Results are shown in the format (mean result) − (input value) ± (standard deviation), in units of 10^{-2}. The standard deviation σ is that of the distribution of fit results; the uncertainty on the mean is $\sigma/\sqrt{100}$. The uncertainty on the standard deviation, $\sigma/\sqrt{200}$, varies between 0.04×10^{-2} and 0.08×10^{-2}.

Table 8 compares the uncertainties obtained with our new method to those from the model-dependent and the model-independent binned method. Studies in [22] show that the unbinned model-independent method introduced there, which is based on projecting the two-dimensional Dalitz plot onto one dimension, results in a statistical uncertainty on γ between that of the model-dependent and the binned method. The authors of [23] report for their Kolmogorov-Smirnov-inspired unbinned method, for similar simulated event numbers as used in our studies, a statistical uncertainty on γ of $\sim 5°$. However, because of the different values assumed for γ and δ_B and differences in the implementation of the amplitude model, comparing the results from [23] with those in table 8 is not straightforward.

JHEP09(2023)007

phase-mod	Method	$\frac{\Delta x_+}{\sigma_{x_+}}$	$\frac{\Delta y_+}{\sigma_{y_+}}$	$\frac{\Delta x_-}{\sigma_{x_-}}$	$\frac{\Delta y_-}{\sigma_{y_-}}$
$f_0 = 0$	QMI	-0.12 ± 0.82	$+0.07 \pm 1.01$	-0.12 ± 1.11	-0.02 ± 1.06
	MD	-0.08 ± 0.82	$+0.13 \pm 1.01$	-0.07 ± 1.06	-0.12 ± 1.01
f_{single}	QMI	$+0.22 \pm 0.89$	-0.07 ± 0.93	$+0.16 \pm 1.08$	$+0.07 \pm 1.28$
	MD	$+1.10 \pm 0.85$	$+3.42 \pm 1.03$	$+0.36 \pm 1.03$	-3.85 ± 1.21
f_{double}	QMI	$+0.17 \pm 0.90$	$+0.07 \pm 0.94$	$+0.02 \pm 0.99$	$+0.13 \pm 1.01$
	MD	$+2.04 \pm 0.87$	$+1.07 \pm 0.95$	-0.93 ± 1.16	-1.81 ± 1.24

Table 7. Pull results from 100 fits with the quasi-model-independent (QMI) and the model-dependent (MD) method, for each of the three phase-modification scenarios. The QMI fit uses a 6^{th} order correction polynomial. Results are shown in the format (mean pull) $\pm$ (standard deviation). The standard deviation is that of the pull distribution (rather than the uncertainty on the mean). The uncertainty on the mean is 0.1, that on the standard deviation is 0.07. The substantial (and expected) biases observed for the model-dependent method for the fits with phase-modification disappear with the QMI method.

	σ_{x_+} $\times 10^2$	σ_{y_+} $\times 10^2$	σ_{x_-} $\times 10^2$	σ_{y_-} $\times 10^2$	σ_{r_B} $\times 10^2$	σ_{δ_B}	σ_γ
binned fit (fixed c_i, s_i)	0.886	1.482	1.189	1.328	0.879	5.33°	5.09°
unbinned QMI	0.780	1.091	0.877	0.945	0.664	4.24°	4.21°
unbinned MD	0.784	1.081	0.878	0.939	0.660	4.19°	4.23°

Table 8. Comparing the QMI method with our implementation of the model-dependent method and the binned method with "optimal" binning (defined in [34]), for the case with no phase modification. The uncertainties given are the average of those reported by the fitter for 100 fits. For the binned fit, we fix c_i and s_i. In contrast to the QMI results, the uncertainties from the binned fit therefore do not include the effect of the finite sample size at the charm threshold, which leads to an additional uncertainty on γ of 1.2° [36].

In our implementation of the binned method, we base the binning on the same amplitude model that we use to generate the simulated data, which should result in a slightly optimistic performance of the binned method. We test all binning schemes defined in [34] and find that the "optimal" binning scheme leads to the best results. In our binned fit, we fix c_i and s_i to their true value (according to our model), so that the uncertainty on γ for the binned method does not include the contribution from the uncertainty on c_i and s_i. The sensitivity studies reported in [37] show that, for the "optimal" binning scheme, taking into account the measurement uncertainties on c_i and s_i leads to an additional uncertainty on γ of 1.2°. This results in a total uncertainty on γ of $5.1^\circ \oplus 1.2^\circ = 5.2^\circ$, which is, on the same simulated signal data, improved to 4.2° by the new method introduced, here.

JHEP09(2023)007

LHCb	$\sigma_{x_+} \cdot 10^2$		$\sigma_{y_+} \cdot 10^2$		$\sigma_{x_-} \cdot 10^2$		$\sigma_{y_-} \cdot 10^2$		σ_γ (°)	
Lumi	MD	bin	MD	bin	MD	bin	MD	bin	MD	bin
×1	0.780	0.886	1.081	1.482	0.878	1.189	0.939	1.328	4.23	5.09
×100	0.078	0.089	0.108	0.149	0.088	0.118	0.093	0.134	0.42	0.52

Table 9. Uncertainties on fit parameters for the model-dependent method and the binned method with fixed c_i, s_i for 1× and 100× the dataset analysed by LHCb in [33]. The uncertainties are the average of those reported by the fitter for fits to 100 pseudoexperiments, generated without backgrounds or detector effects. The statistical uncertainty on the mean of σ_γ ranges from 1% to 3% of its value.

Lumi scenario:						
LHCb	BES III	$\sigma_{x_+} \cdot 10^2$	$\sigma_{y_+} \cdot 10^2$	$\sigma_{x_-} \cdot 10^2$	$\sigma_{y_-} \cdot 10^2$	σ_γ (°)
×1	×1	0.780	1.091	0.877	0.945	4.21
×1	×10	0.773	1.062	0.866	0.924	4.18
×100	×1	0.079	0.122	0.090	0.104	0.45
×100	×10	0.078	0.115	0.089	0.099	0.43

Table 10. Uncertainties on fit parameters for the QMI method, for scenarios with 1× and 100× the dataset analysed by LHCb in [33], and 1× and 10× the dataset analysed by BES III in [36, 37]. The uncertainties are the average uncertainty reported by the fitter for ∼ 100 simulated datasets, generated without backgrounds or detector effects. The statistical uncertainty on the mean of σ_γ is ∼ 1% of its value.

4.2.3 Alternative sample sizes

For the studies above, we used sample sizes corresponding to those reported in recent publications by BES III [36, 37] and LHCb [33]. Here we consider possible future datasets that are considerably larger, 10× as large for BES III and 100× as large for LHCb. The results for the QMI method are presented in table 10. The results for the model-dependent method and the binned method with fixed c_i, s_i are given in table 9. The results for the binned method, with fixed c_i, s_i, represent the best possible uncertainty on γ that can be reached with this method in the limit of infinitely large threshold data sets, given the 8-bin-pair binning scheme and other parameters used in this study. It is possible that a finer binning would improve the uncertainty for the larger data set.

The uncertainties for all methods studied scale to a good approximation with $1/\sqrt{N_B}$, where N_B is the number of $B^\pm \to DK^\pm, D \to K^0_S\pi^+\pi^-$ events. That this is so for the QMI method is not a priori obvious, given that it depends also on $\psi(3770) \to D\overline{D}$ (i.e. CLEO-c or BES III) data. This suggests that the QMI method is very efficient in extracting information on $\delta_D(s_+, s_-)$ not only from threshold data, but also from $B^\pm \to DK^\pm, D \to K^0_S\pi^+\pi^-$.

For the 1×LHCb scenario, the lack of significant improvement in the uncertainty on γ for the 10× larger BES III sample is consistent with the earlier observation that the QMI method with the 1×LHCb and 1×BES III scenario already achieves effectively the

JHEP09(2023)007

same statistical precision as the model-dependent method (i.e. the best possible for the $B^\pm \to DK^\pm, D \to K^0_S\pi^+\pi^-$ dataset). For the 100×LHCb dataset, the larger BES III sample improves the precision slightly from 0.45° to 0.43°, compared to the benchmark of 0.42° set by the model-dependent method.

Overall, our results indicate that, with the QMI method introduced here, the statistical precision on γ in $B^\pm \to DK^\pm, D \to K^0_S\pi^+\pi^-$ remains close to the optimum defined by the model-dependent method not only with current datasets, but also much larger $B^\pm \to DK^\pm$ datasets that might become available in the future.

5 Conclusion

We have introduced a novel unbinned quasi model-idependent (QMI) method for the measurement of γ in $B^\pm \to DK^\pm$ decays, with input from quantum-correlated charm threshold data. The method uses a polynomial to correct the phase of the D meson's decay amplitude model in an unbinned, model-independent way.

We studied the performance of the method using simulated $B^\pm \to DK^\pm, D \to K^0_S\pi^+\pi^-$ and $\psi(3770) \to D\overline{D}$ signal events. The method produces unbiased results for cases where discrepancies between the assumed amplitude model and the true model produce large biases in a model-dependent measurement. For realistic current and plausible future sample sizes, the method achieves a statistical precision on γ that is effectively the same as the optimum defined by the model-dependent method, without suffering from the systematic uncertainty associated with the amplitude model. The statistical uncertainty is significantly better than that of the binned model-independent method currently in use.

We expect that the QMI method will also be beneficial in the study of charm mixing and the study of phases of decay amplitudes across the Dalitz plot.

Acknowledgments

J. Lane and E. Gersabeck have received support by the Royal Society (U.K.), J. Rademacker from STFC (U.K.); we express our gratitude. We thank Dr Tim Evans for the development and support of the Amplitude Analysis framework `AmpGen` [41], upon which our software is built. We thank Prof Marco Gersabeck, Dr Martha Hilton (now at the Institute of Physics (U.K.)), Dr Mark Williams (now at the University of Edinburgh), Dr Florian Reiss, and Dr David Friday from the University of Manchester; Prof Tim Gershon from the University of Warwick; and Jozie Cottee Meldrum from the University of Bristol for their insightful feedback. We are indebted to the participants of the Charming Clues for Existence workshop (2022) at the Munich Institute for Astro and Particle Physics (supported by the German Research Foundation, DFG, project EXC-2094 — 390783311) for helpful comments and discussions.

JHEP09(2023)007

References

[1] M. Gronau and D. Wyler, *On determining a weak phase from CP asymmetries in charged B decays*, *Phys. Lett. B* **265** (1991) 172 [INSPIRE].

[2] M. Gronau and D. London, *How to determine all the angles of the unitarity triangle from $B_d^0 \to DK_S$ and $B_s^0 \to D^0\phi$*, *Phys. Lett. B* **253** (1991) 483 [INSPIRE].

[3] A. Bondar, *Proceedings of BINP special analysis meeting on Dalitz analysis*, unpublished, 24–26 September 2002.

[4] A. Giri, Y. Grossman, A. Soffer and J. Zupan, *Determining γ using $B^\pm \to DK^\pm$ with multibody D decays*, *Phys. Rev. D* **68** (2003) 054018 [hep-ph/0303187] [INSPIRE].

[5] BELLE collaboration, *Measurement of ϕ_3 with Dalitz plot analysis of $B^\pm \to D^{(*)}K^\pm$ decay*, *Phys. Rev. D* **70** (2004) 072003 [hep-ex/0406067] [INSPIRE].

[6] D. Atwood, I. Dunietz and A. Soni, *Enhanced CP violation with $B \to KD^0(\bar{D}^0)$ modes and extraction of the CKM angle γ*, *Phys. Rev. Lett.* **78** (1997) 3257 [hep-ph/9612433] [INSPIRE].

[7] J. Brod and J. Zupan, *The ultimate theoretical error on γ from $B \to DK$ decays*, *JHEP* **01** (2014) 051 [arXiv:1308.5663] [INSPIRE].

[8] LHCb collaboration, *Simultaneous determination of the CKM angle γ and parameters related to mixing and CP violation in the charm sector*, LHCb-CONF-2022-003, CERN, Geneva, Switzerland (2022).

[9] LHCb collaboration, *Simultaneous determination of CKM angle γ and charm mixing parameters*, *JHEP* **12** (2021) 141 [arXiv:2110.02350] [INSPIRE].

[10] LHCb collaboration, *Framework TDR for the LHCb upgrade: technical design report*, CERN-LHCC-2012-007, CERN, Geneva, Switzerland (2012).

[11] BELLE-II collaboration, *Belle II technical design report*, arXiv:1011.0352 [INSPIRE].

[12] LHCb collaboration, *Framework TDR for the LHCb upgrade II*, CERN-LHCC-2021-012, CERN, Geneva, Switzerland (2021).

[13] LHCb collaboration, *Physics case for an LHCb upgrade II — opportunities in flavour physics, and beyond, in the HL-LHC era*, arXiv:1808.08865 [INSPIRE].

[14] N. Cabibbo, *Unitary symmetry and leptonic decays*, *Phys. Rev. Lett.* **10** (1963) 531 [INSPIRE].

[15] M. Kobayashi and T. Maskawa, *CP violation in the renormalizable theory of weak interaction*, *Prog. Theor. Phys.* **49** (1973) 652 [INSPIRE].

[16] A. Bondar, A. Poluektov and V. Vorobiev, *Charm mixing in the model-independent analysis of correlated $D^0\bar{D}^0$ decays*, *Phys. Rev. D* **82** (2010) 034033 [arXiv:1004.2350] [INSPIRE].

[17] D. Atwood and A. Soni, *Role of charm factory in extracting CKM phase information via $B \to DK$*, *Phys. Rev. D* **68** (2003) 033003 [hep-ph/0304085] [INSPIRE].

[18] A. Bondar and A. Poluektov, *Feasibility study of model-independent approach to ϕ_3 measurement using Dalitz plot analysis*, *Eur. Phys. J. C* **47** (2006) 347 [hep-ph/0510246] [INSPIRE].

[19] S. Harnew and J. Rademacker, *Charm mixing as input for model-independent determinations of the CKM phase γ*, *Phys. Lett. B* **728** (2014) 296 [arXiv:1309.0134] [INSPIRE].

[20] S. Harnew and J. Rademacker, *Model independent determination of the CKM phase γ using input from D^0-$\bar{D}^0$ mixing*, *JHEP* **03** (2015) 169 [arXiv:1412.7254] [INSPIRE].

JHEP09(2023)007

[21] M. Nayak et al., *First determination of the CP content of $D \to \pi^+\pi^-\pi^0$ and $D \to K^+K^-\pi^0$*, *Phys. Lett. B* **740** (2015) 1 [arXiv:1410.3964] [INSPIRE].

[22] A. Poluektov, *Unbinned model-independent measurements with coherent admixtures of multibody neutral D meson decays*, *Eur. Phys. J. C* **78** (2018) 121 [arXiv:1712.08326] [INSPIRE].

[23] J.V. Backus et al., *Toward extracting γ from $B \to DK$ without binning*, arXiv:2211.05133 [INSPIRE].

[24] C.C. Meca and J.P. Silva, *Detecting new physics contributions to the D^0-$\bar{D}^0$ mixing through their effects on B decays*, *Phys. Rev. Lett.* **81** (1998) 1377 [hep-ph/9807320] [INSPIRE].

[25] J.P. Silva and A. Soffer, *Impact of D^0-$\bar{D}^0$ mixing on the experimental determination of γ*, *Phys. Rev. D* **61** (2000) 112001 [hep-ph/9912242] [INSPIRE].

[26] Y. Grossman, A. Soffer and J. Zupan, *The effect of D-$\bar{D}$ mixing on the measurement of γ in $B \to DK$ decays*, *Phys. Rev. D* **72** (2005) 031501 [hep-ph/0505270] [INSPIRE].

[27] M. Rama, *Measurement of strong phases, D-$\bar{D}$ mixing, and CP violation using quantum correlation at charm threshold*, *Front. Phys. (Beijing)* **11** (2016) 111404 [INSPIRE].

[28] Belle collaboration, *First measurement of ϕ_3 with a model-independent Dalitz plot analysis of $B^\pm \to DK$, $D \to K^o_s\pi\pi$ decay*, *Phys. Rev. D* **85** (2012) 112014 [arXiv:1204.6561] [INSPIRE].

[29] Belle collaboration, *First model-independent Dalitz analysis of $B^0 \to DK^{*0}$, $D \to K^0_S\pi^+\pi^-$ decay*, *PTEP* **2016** (2016) 043C01 [arXiv:1509.01098] [INSPIRE].

[30] Belle and Belle-II collaborations, *Combined analysis of Belle and Belle II data to determine the CKM angle ϕ_3 using $B^+ \to D(K^0_S h^- h^+)h^+$ decays*, *JHEP* **02** (2022) 063 [*Erratum ibid.* **12** (2022) 034] [arXiv:2110.12125] [INSPIRE].

[31] LHCb collaboration, *A model-independent Dalitz plot analysis of $B^\pm \to DK^\pm$ with $D \to K^0_S h^+h^-$ ($h = \pi, K$) decays and constraints on the CKM angle γ*, *Phys. Lett. B* **718** (2012) 43 [arXiv:1209.5869] [INSPIRE].

[32] LHCb collaboration, *Measurement of the CKM angle γ using $B^\pm \to DK^\pm$ with $D \to K^0_S\pi^+\pi^-$, $K^0_S K^+K^-$ decays*, *JHEP* **08** (2018) 176 [*Erratum ibid.* **10** (2018) 107] [arXiv:1806.01202] [INSPIRE].

[33] LHCb collaboration, *Measurement of the CKM angle γ in $B^\pm \to DK^\pm$ and $B^\pm \to D\pi^\pm$ decays with $D \to K^0_S h^+h^-$*, *JHEP* **02** (2021) 169 [arXiv:2010.08483] [INSPIRE].

[34] CLEO collaboration, *Model-independent determination of the strong-phase difference between D^0 and $\bar{D}^0 \to K^0_{S,L}h^+h^-$ ($h = \pi, K$) and its impact on the measurement of the CKM angle γ/ϕ_3*, *Phys. Rev. D* **82** (2010) 112006 [arXiv:1010.2817] [INSPIRE].

[35] CLEO collaboration, *First model-independent determination of the relative strong phase between D^0 and $\bar{D}^0 \to K^0_{(S)}\pi^+\pi^-$ and its impact on the CKM angle γ/ϕ_3 measurement*, *Phys. Rev. D* **80** (2009) 032002 [arXiv:0903.1681] [INSPIRE].

[36] BESIII collaboration, *Determination of strong-phase parameters in $D \to K^0_{S,L}\pi^+\pi^-$*, *Phys. Rev. Lett.* **124** (2020) 241802 [arXiv:2002.12791] [INSPIRE].

[37] BESIII collaboration, *Model-independent determination of the relative strong-phase difference between D^0 and $\bar{D}^0 \to K^0_{S,L}\pi^+\pi^-$ and its impact on the measurement of the CKM angle γ/ϕ_3*, *Phys. Rev. D* **101** (2020) 112002 [arXiv:2003.00091] [INSPIRE].

JHEP09(2023)007

[38] LHCb collaboration, *Measurement of the CKM angle γ with $B^{\pm} \to D[K^{\mp}\pi^{\pm}\pi^{\pm}\pi^{\mp}]h^{\pm}$ decays using a binned phase-space approach*, *JHEP* **07** (2023) 138 [arXiv:2209.03692] [INSPIRE].

[39] BABAR and BELLE collaborations, *Measurement of $\cos 2\beta$ in $B^0 \to D^{(*)}h^0$ with $D \to K^0_S\pi^+\pi^-$ decays by a combined time-dependent Dalitz plot analysis of BaBar and Belle data*, *Phys. Rev. D* **98** (2018) 112012 [arXiv:1804.06153] [INSPIRE].

[40] J. Back et al., *LAURA^{++}: a Dalitz plot fitter*, *Comput. Phys. Commun.* **231** (2018) 198 [arXiv:1711.09854] [INSPIRE].

[41] T. Evans, *AmpGen Gitlab repository*, https://gitlab.com/tevans1260/AmpGen.

[42] HEAVY FLAVOR AVERAGING GROUP and HFLAV collaborations, *Averages of b-hadron, c-hadron, and τ-lepton properties as of* 2021, *Phys. Rev. D* **107** (2023) 052008 [arXiv:2206.07501] [INSPIRE].

[43] F. James and M. Roos, *Minuit: a system for function minimization and analysis of the parameter errors and correlations*, *Comput. Phys. Commun.* **10** (1975) 343 [INSPIRE].

JHEP09(2023)007